Thermodynamic Study of the Binding of the Tandem-SH2 Domain of the Syk Kinase to a Dually Phosphorylated ITAM Peptide: Evidence for Two Conformers†

Richard A. Grucza,‡ Klaus Fütterer,‡ Andrew C. Chan,§,|| and Gabriel Waksman*,‡

Department of Biochemistry and Molecular Biophysics, Departments of Medicine and Pathology, and Howard Hughes Medical Institute, Washington University School of Medicine, Campus Box 8231, 660 South Euclid Avenue, St. Louis, Missouri 63110

Received December 21, 1998; Revised Manuscript Received March 4, 1999

ABSTRACT: The cytosolic tyrosine kinase Syk is recruited to immune cell receptors via interactions of its tandem-SH2 domain with tyrosine-phosphorylated sequences called immune receptor tyrosine activation motifs (ITAMs). We have characterized the binding of the tandem-SH2 domain of Syk (Syk-tSH2) to a dually phosphorylated peptide derived from the ITAM of the T cell receptor CD3-ϵ subunit. The CD3-ϵ peptide binds with an affinity of 18−81 nM at 150 mM NaCl over the 4.5−30 °C temperature range that was studied. The enthalpy of binding, ΔH°_{obs}, shows an unusual nonlinear dependence on temperature, suggesting the possibility of a temperature-dependent conformational equilibrium coupled to binding. This hypothesis was tested and confirmed by examining the temperature dependence of (1) the on-rate constant for binding and (2) the fluorescence of Syk-tSH2 and its CD3-ϵ peptide complex. The ΔH°_{obs}, K_{obs}, fluorescence, and kinetic data are all well described by a model incorporating the hypothesized conformational equilibrium. Circular dichroism spectra at various temperatures indicate that the conformational change is not due to a partial unfolding of the protein. We suggest that the conformational equilibrium enables Syk-tSH2 to exhibit flexibility in its binding modality, which may be necessitated by Syk's involvement in a wide variety of signal tranduction pathways.

The Syk family of kinases is comprised of two non-receptor protein tyrosine kinases (PTKs), Syk and ZAP-70, which play important roles in signaling by antigen and immunoglobin (Ig) receptors (reviewed in refs *1*−*4*). The absence of either ZAP-70 or Syk results in arrested T and B cell development and in functional defects for a variety of immune receptors, including the T cell antigen receptor (TCR), the B cell antigen receptor (BCR), and receptors for IgG and IgE (*5*−*7*; reviewed in refs *3* and *8*). Both Syk and Zap-70 consist of two adjacent src homology 2 (SH2) domains separated from the C-terminal kinase domain by a linker region (*1*).

The sites on the receptors which mediate the interactions with the Syk family kinases are known as immunoreceptor tyrosine activation motifs (ITAMs) and have the consensus sequence Yxx(L/I)-$x_{7/8}$-Yxx(L/I) (*9*, *10*). Phosphorylation of both tyrosines within the ITAM by the membrane-associated Src family kinases is required for recruitment of ZAP-70 and Syk to the immune receptor subunits (*11*−*15*). ITAM phosphorylation results in a high-affinity binding site for the tandem-SH2 domain. Disruption of phosphorylation on either tyrosine residue within the ITAM results in a considerably attenuated interaction and in an inactive immune receptor (*11*, *13*, *15*, *16*).

Although both Syk and ZAP-70 PTKs are involved in immune receptor signaling, they differ with respect to the variety of pathways in which they are involved and the identity of the ITAMs with which they interact. While ZAP-70 is restricted to signaling in T cells and natural killer (NK) cells, Syk is more ubiquitously expressed among hematopoietic cells and has been shown to be activated not only by a wide variety of immune response receptors but also by nonimmune receptors such as those for cytokines (*17*, *18*), integrins (*19*, *20*), thrombin (*21*), and G protein-coupled receptors (*22*). Moreover, in the non-immune receptor-dependent signaling pathways in which Syk is involved, the interactions of Syk with the ITAM sequences may not require the involvement of both SH2 domains. For example, the C-terminal SH2 domain is not required for Syk activation by the $\alpha_{IIb}\beta_3$ integrin receptor, while the N-terminal SH2 domain is not required for activation of the MAP kinase pathway by the G_q-coupled muscarinic acetylcholine receptor (*19*, *22*). Finally, Syk has been shown to bind ITAM sequences which deviate from the canonical consensus sequence in the insertion of four to five residues between the two tyrosines (*17*, *23*).

Although the more ubiquitous role of Syk compared to that of Zap-70 may be explained by the distinct patterns of expression of these two kinases, it may also be the result of differences in ITAM recognition by the tandem-SH2 domains of the two proteins. The second possibility was recently explored by Fütterer et al. (*24*), who described the crystal structure of a complex of the Syk tandem-SH2 domain bound

† This work was supported by funds from Washington University School of Medicine.

* To whom correspondence should be addressed: Department of Biochemistry and Molecular Biophysics, Washington University School of Medicine, 660 S. Euclid Ave., Campus Box 8231, St. Louis, MO 63110. Telephone: (314) 362-4562. Fax: (314) 362-7183. E-mail: waksman@biochem.wustl.edu.

‡ Department of Biochemistry and Molecular Biophysics.

§ Departments of Medicine and Pathology.

|| Howard Hughes Medical Institute.

10.1021/bi9829938 CCC: $18.00
Published on Web 03/31/1999

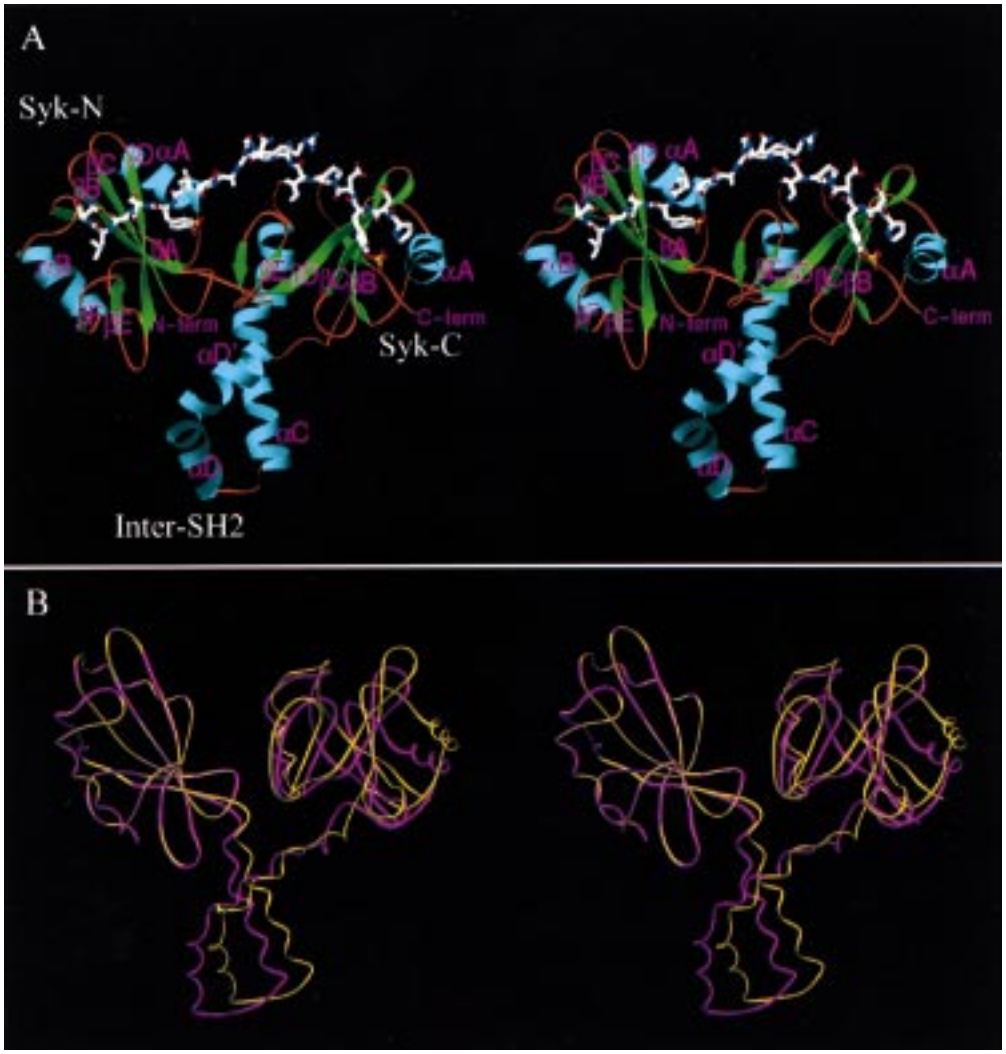

FIGURE 1: Views of the crystal structure of the Syk tandem-SH2 domain bound to the CD3-ϵ peptide. (A) Stereo-ribbon diagram of the tandem-SH2 domain of Syk in a complex with the CD3-ϵ ITAM peptide. The ITAM peptide is shown in a ball-and-stick representation with carbon atoms in white, nitrogen atoms in blue, and oxygen atoms in red. Secondary structural elements are labeled according to the notation adopted in Fütterer et al. (*24*) and colored green for β-strands, cyan for α-helices, and orange for loops and turns. Syk-N and Syk-C refer to the N- and C-terminal SH2 domains, respectively. (B) Conformational flexibility in CD3-ϵ-ligated Syk-tSH2. Two molecules of the asymmetric unit of the Syk-tSH2−CD3-ϵ complex crystal (*24*) were superimposed with respect to the N-terminal SH2 domain (on the left). The orientation is the same as in panel A. These two conformations represent the two extremes of the conformational change which affects the C-terminal SH2 domain (on the right).

to a dually phosphorylated ITAM peptide (Figure 1). The asymmetric unit is comprised of six copies of the ligated protein, thereby providing six independent views of this structure. A surprising flexibility in the relative orientation of the two SH2 domains was revealed. Also, it was shown that the two SH2 domains of Syk, in contrast to those of ZAP-70, do not form a common C-terminal phosphotyrosine-binding site, suggesting that unlike ZAP-70, the two SH2 domains of Syk can function as independent units. These two observations may account for the differences in function between ZAP-70 and Syk. Although the crystal structures of Fütterer et al. (*24*) are evidence for conformational flexibility in the tandem-SH2 domain of Syk, any conformational changes in solution and their degree of coupling to ITAM binding remain undocumented.

Calorimetric studies have been crucial in dissecting the interactions between SH2 domains and phosphotyrosyl peptides (*25*−*32*). Calorimetric measurements give a direct evaluation of the binding enthalpy ($\Delta H°$) which, when studied as a function of temperature to extract the heat capacity change ($\Delta C_p°$), helps to discern whether binding occurs via a rigid-body or an induced-fit mechanism (*33*). Moreover, the temperature dependence of the $\Delta C_p°$, which is most precisely assessed by calorimetry rather than by van't Hoff analysis, can determine if binding is linked to a pre-existing conformational equilibrium (*34*, *35*). A detailed understanding of the energetics of tyrosine-phosphorylated peptide recognition by SH2 domains would greatly facilitate drug design efforts; SH2 domains have been the targets of intensive pharmacological research (*36*), and recently, a specific inhibitor of the interaction of Syk with the Fcϵ receptor I, apparently involving the SH2 domains, has been reported (*37*).

In the study presented here, we examine the thermodynamics of binding of the tandem-SH2 domain of Syk to a dually phosphorylated ITAM peptide and show that the binding process is complicated by an apparent ligation-coupled conformational change. This conclusion is the result of combined spectroscopic and calorimetric studies in which the temperature-dependent thermodynamics of binding of the

tandem-SH2 domain of Syk were evaluated and is the first of this type involving a tandem-SH2 domain. We propose that the observed conformational equilibrium is related to the conformational sampling seen in the bound state by Fütterer et al. (*24*) using X-ray crystallography.

MATERIALS AND METHODS

Protein Expression and Purification. The Syk tandem-SH2 domain (Syk-tSH2) was expressed and purified as described previously (*24*). The purity was assessed by SDS−PAGE and determined to be >95%. Prior to all experiments, exhaustive dialysis was carried out in a standard experimental buffer consisting of 50 mM Hepes, 150 mM NaCl, 150 mM glycine, 1 mM EDTA, and 5 mM β-mercaptoethanol at pH 7.5. The protein concentration was determined via the absorbance at 280 nM using an extinction coefficient of 34 425 M^{-1} cm^{-1} calculated from the amino acid sequence (*38*) and confirmed by stoichiometric titration.

Tyrosine Phosphopeptides. The sequence of the CD3-ϵ phosphopeptide used in this study is Ac-PDpYEPIRKGQRD-LpYSGLNQR-NH_2, where pY denotes a phosphotyrosine (see ref *24* for details). The doubly tyrosine-phosphorylated peptide was obtained from Quality Controlled Biochemicals (Hopkinton, MA). Peptide concentrations were determined using an extinction coefficient of 1304 M^{-1} cm^{-1} at 267 nm, based on an extinction coefficient for phosphotyrosine of 652 M^{-1} cm^{-1} (*39*). Excess salts were removed from the peptide by dialysis against the standard experimental buffer.

Isothermal Calorimetry. Calorimetric measurements were conducted using an OMEGA isothermal titration calorimeter from Microcal, Inc. (Northhampton, MA). All the reagents that were used in the experiments were degassed for at least 20 min. Batch calorimetry in which the enthalpy of binding was measured with a single injection of ligand into protein was employed. Typically, a solution of 2.5−5 μM protein was equilibrated in the calorimeter cell ($V = 1.35$ mL). The injection syringe contained solutions of 350−800 μM ligand which was injected in volumes of 15−30 μL. The final ligand:protein molar ratio was between 1.5 and 2.0 for all the experiments that were conducted, corresponding to ≥98.5% saturation. Ligand-to-buffer blank injections were carried out for each enthalpy measurement. The heat of reaction for each run was determined by integrating the single peak, subtracting the heat of the ligand-to-buffer blank, and dividing by the number of moles of complex that formed. The dependence of the enthalpy of binding on temperature was studied over the 7.5−30 °C range. The upper limit of this temperature range was chosen on the basis of the fluorescence temperature scans (see below).

Fluorescence Titrations and the Temperature Dependence of the Fluorescence Signal. Fluorescence titrations were carried out to determine the binding constants. The titrations were conducted in an SLM 8000 spectrofluorimeter equipped with a water-jacketed cell turret which was used to control the temperature. An excitation wavelength of 289.5 nm was used, a wavelength at which phosphotyrosine exhibits negligible absorbance. In quartz cuvettes, 2.5 mL solutions of 300−500 nM Syk-tSH2 were titrated by incremental addition of peptide solutions at concentrations of 40−70 μM. Solutions were incubated for ≥3 min prior to reading the fluorescence intensity. The emission wavelength was selected using a monochromator and was centered at 340 nm, the wavelength at which the intensity difference between the ligated and unligated forms of Syk-tSH2 is maximal. Slit widths were 1 or 2 mm for excitation and 8 or 16 mm for emission. Binding constants were determined in the standard experimental buffer at varying temperatures ranging from 4.5 to 30 °C. Plots of normalized fluorescence intensity versus total ligand concentration were prepared for each titration. Corrections for the loss of signal due to photobleaching (<0.5% of the overall fluorescence signal) were applied to the intensity measurements. Data were fit to a single-site binding model. The derived binding constants were found to be independent of protein concentration (data not shown).

Fluorescence was also used as a conformational probe of the unligated and ligated Syk-tSH2 proteins. Measurements were carried out using a 450 nM protein solution. The CD3-ϵ−ITAM complex was formed by adding a 20-fold excess of peptide. The fluorescence intensity was measured as a function of temperature over the range of 5−33 °C for the unligated Syk-tSH2 and 3.7−36 °C for the CD3-ϵ complex. At various temperature points, samples were cooled to the starting temperature to ensure that no loss of signal had occurred due to adsorption to the cuvette. Temperatures at which this occurred constituted the upper limit of the temperature scans. Fluorescence readings were taken using the excitation and emission wavelengths listed above.

Stopped-Flow Kinetics of Binding. Kinetics of binding were studied using an Applied Photophysics stopped-flow apparatus (Surrey, U.K.) in the fluorescence mode with a cell with a path length of 0.2 cm. Two 2.5 mL drive syringes were used to mix stock solutions, which consisted of 1 μM Syk-tSH2 and 5 μM CD3-ϵ peptide. One thousand data points were collected over a time interval of at least $5/k_{obs}$, where k_{obs} is the observed on-rate constant; this interval ranged from 50 to 500 ms. The excitation wavelength was 289.5 nm, and a 305 nm cutoff filter was used for emission. For each data set, five individual runs were performed and averaged prior to analysis. The temperature of the apparatus was controlled with an attached water bath.

Circular Dichroism. Circular dichroism spectra were recorded on a Jasco-J715 spectropolarimeter. Samples of Syk-tSH2 at a concentration of 19 μM (0.58 mg/mL) in the standard buffer were incubated in a water-jacketed cell with a path length of 1.0 cm. Spectra were taken from 305 to 270 nm at temperatures ranging from 10 to 30 °C.

Data Fitting. All nonlinear least-squares fitting was performed with the program Scientist (Micromath, Salt Lake City, UT). Reported errors for fitted values represent 95% confidence intervals, computed in Scientist using the support plane method. When data sets collected from multiple techniques were simultaneously fit, each data point was weighted by a factor of the inverse of the estimated standard error. For the binding enthalpies, the uncertainty was estimated by calculating the standard deviation for each temperature at which duplicate measurements were taken (temperatures within 0.3 K were taken to be identical). These standard deviations showed no correlation with the magnitude of the measured enthalpy, so the average of the standard deviations was taken to be a measure of the absolute uncertainty for each measurement. Confidence intervals (95%) were calculated on the basis of this averaged standard

Scheme 1: Proposed Model Describing the Thermodynamic Cycle Linking Syk-tSH2 Ligand Binding to Conformation and Temperature[a]

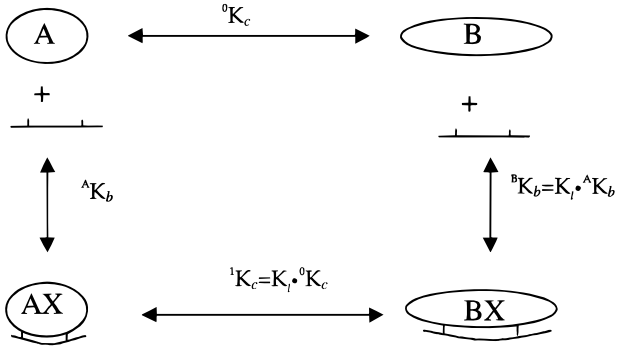

[a] A and B represent the two conformers of Syk-tSH2 in the unligated states; AX and BX are the ligated forms. The conformational equilibria favor the B forms of Syk-tSH2 as temperature increases, but the A form preferentially binds to ligand, thus driving the equilibrium toward the AX form upon ligand binding. In this scheme and throughout the text, superscripts preceding thermodynamic variables represent values that are specific to a state of the protein: 0 and 1 for unligated and ligated, respectively, and A and B for the respective conformers. Subscripts denote the process with which the variable is associated: b for binding, c for the conformational change, and l for the linkage of the two processes. Observed properties reflecting a combination of intrinsic processes are indicated by the subscript obs. Binding equilibrium constants (K_{obs} and K_b) are described as association constants rather than dissociation constants, unless otherwise indicated.

deviation. For K_{obs}, uncertainty estimates were taken from the fitted titration curves, while for F_{obs}, the uncertainty was estimated from replicate measurements.

THEORY

Several lines of evidence point to a model in which unligated Syk-tSH2 undergoes a temperature-induced conformational change which is linked to ITAM ligand binding. This hypothesis is illustrated in Scheme 1 as a two-conformer thermodynamic cycle. In this section, we develop the equations that describe the behavior expected from this model for each of the four observables we have monitored as functions of temperatures, i.e., the binding constant $K_{obs}(T)$, the binding enthalpy $\Delta H^\circ_{obs}(T)$, the on-rate constant $k_{obs}(T)$, and the intrinsic fluorescence signal $F_{obs}(T)$. We also describe the parameters to be determined by nonlinear least-squares fitting.

Thermodynamic Parameters as Functions of Temperature. According to Scheme 1, the observed equilibrium binding constant is a conformer population-weighted average of the intrinsic binding constants for the two forms:

$$K_{obs}(T) = \frac{[BX] + [AX]}{([A] + [B]) \times x} = {}^AK_b(T)\left[\frac{1}{1 + {}^0K_c(T)}\right] + {}^BK_b(T)\left[\frac{{}^0K_c(T)}{1 + {}^0K_c(T)}\right] \quad (1)$$

where x represents free ligand concentration, $^AK_b(T)$ is the equilibrium binding constant for the A + x → AX binding event, $^BK_b(T)$ is the equilibrium binding constant for the B + x → BX binding event, and $^0K_c(T)$ is the equilibrium constant for the A ↔ B conformational transition (see the footnote of Scheme 1 for a description of the notation of thermodynamic variables). Each equilibrium constant is a function of temperature governed by standard thermodynamic relationships for processes involving a significant ΔC_p° (described below).

In accordance with the first law of thermodynamics, the ratio $^BK_b(T)/^AK_b(T)$ must be the same as $^1K_c(T)/^0K_c(T)$, where $^1K_c(T)$ is the conformational equilibrium constant for the AX ↔ BX transition. This ratio is defined as $K_l(T)$:

$$K_l(T) = \frac{{}^BK_b(T)}{{}^AK_b(T)} = \frac{{}^1K_c(T)}{{}^0K_c(T)} = \frac{[BX][A]}{[AX][B]} \quad (2)$$

Thus, $K_l(T)$ is an equilibrium constant for a hypothetical AX + B ↔ BX + A transition; a value for K_l of <1 would indicate that A is the preferentially binding conformer, and a K_l of >1 would mean that B is the preferentially binding conformer. If $K_l = 0$, the BX form is not populated and the conversion to AX is complete upon ligation.

Using the Gibbs−Helmholtz relation $[[\partial(\ln K)/\partial(T)]_p = \Delta H^\circ/RT^2]$, an expression for the observed enthalpy of binding can be derived from eq 1:

$$\Delta H^\circ_{obs}(T) = {}^A\Delta H^\circ_b(T) - {}^0\Delta H^\circ_c(T)\frac{{}^0K_c(T)}{1 + {}^0K_c(T)} + [{}^0\Delta H^\circ_c(T) + \Delta H^\circ_l(T)]\frac{K_l(T){}^0K_c(T)}{1 + K_l(T){}^0K_c(T)} \quad (3)$$

where $^A\Delta H^\circ_b(T)$, $^0\Delta H^\circ_c(T)$, and $\Delta H^\circ_l(T)$ are the intrinsic enthalpies related to the equilibrium constants $^AK_b(T)$, $^0K_c(T)$, and $K_l(T)$ for binding to the reference state (the A conformer), the conformational change, and the linkage of the two, respectively.

Fluorescence as a Function of Temperature. As a consequence of the presence of two conformers in equilibrium, any spectroscopic properties of Syk-tSH2 represent contributions from each of the two conformers. As discussed below in the Results, we expect that a plot of $\log(F_{obs})$ versus inverse temperature will yield a straight line for a single conformer. Thus, if two conformers with distinct fluorescent signals are present, the total fluorescence can be described by the following expression:

$$\log(F_{obs}) = \frac{1}{1 + {}^iK_c(T)}\left(\frac{m_A}{T} + b_A\right) + \frac{{}^iK_c(T)}{1 + {}^iK_c(T)}\left(\frac{m_B}{T} + b_B\right) \quad (4)$$

where m_A and m_B are the slopes for the variation of $\log(F_{obs})$ with inverse temperature for the A and B conformers, b_A and b_B are their intercepts, respectively, and $^iK_c(T)$ is the conformational equilibrium constant for the species in question, i.e., unligated Syk-tSH2 or the CD3-ϵ−Syk-tSH2 complex.

Apparent On-Rate for Binding, k_{obs}, as a Function of Temperature. If it is hypothesized that the single observed fast phase in the stopped-flow kinetic experiments represents two processes with rate constants with similar magnitudes such that the two exponentials cannot be resolved by nonlinear least-squares fitting, then the single observed rate constant would be approximately a conformer population-

weighted average of the two intrinsic binding rate constants or

$$k_{obs}(T) = W_A \frac{1}{1 + {}^{i}K_c(T)} k_A(T) + W_B \frac{{}^{i}K_c(T)}{1 + {}^{i}K_c(T)} k_B(T) \quad (5)$$

where $k_A(T)$ and $k_B(T)$ are the intrinsic binding rate constants for the A and B forms, respectively, and W_A and W_B are weighting factors that account for the relative changes in the spectroscopic signal accompanying each microscopic process, respectively.

Parameters Derived from the Fitting Procedure. The experimentally observed K_{obs}, ΔH°_{obs}, and F_{obs} data were fitted to eqs 1, 3, and 4, respectively (see the Results). These equations contain the three equilibrium constants governing the thermodynamic cycle of Scheme 1 [${}^{A}K_b(T)$, ${}^{0}K_c(T)$, and $K_l(T)$] and the enthalpies associated with them. For processes that involve a significant $\Delta C_p{}^\circ$, the equilibrium constant, enthalpy, and entropy of the process are functions of temperature according to the three temperature-independent parameters T_{hi} (temperature at which the enthalpy of the process is zero), T_{si} (temperature at which the entropy of the process is zero), and ΔC°_{pi}:

$$\ln K_i(T) = \frac{-\Delta G_i(T)}{RT} = \frac{-\Delta C^\circ_{pi}}{R}\left(1 - \frac{T_{hi}}{T} + \ln\frac{T}{T_{si}}\right) \quad (6.1)$$

$$\Delta H^\circ_i(T) = \Delta C^\circ_{pi}(T - T_{hi}) \quad (6.2)$$

$$\Delta S^\circ_i(T) = \Delta C^\circ_{pi} \ln\left(\frac{T}{T_{si}}\right) \quad (6.3)$$

where the subscript i identifies the process (b, c, or l).

In initial attempts to fit the data, it became clear that the large number of variables and the correlations among them made it impossible to uniquely determine all the parameters, and it was necessary to make the following simplifying approximations. (1) Because direct measurements of ΔC°_{pc} values could not be taken (see the Discussion), the enthalpies of the A ↔ B and AX ↔ BX transitions were approximated to be temperature-independent, i.e., ${}^{0}\Delta C^\circ_{pc} = \Delta C^\circ_{pl} = 0$. The validity of this approximation was subsequently tested and borne out by data simulation (data not shown). Thus, the temperature dependences of the conformational equilibrium constant, ${}^{0}K_c(T)$, and of the linkage parameter, $K_l(T)$, may be rewritten as

$$\ln {}^{0}K_c(T) = \frac{-{}^{0}\Delta H^\circ_c}{RT} + \frac{{}^{0}\Delta S^\circ_c}{R} \quad (7.1)$$

$$\ln K_i(T) = \frac{-\Delta H^\circ_l}{RT} + \frac{\Delta S^\circ_l}{R} \quad (7.2)$$

Since, for a conformational change, it is often informative to determine the temperature at which $K_c = 1$ (i.e., the midpoint of the conformational transition, T_m), eqs 7.1 and 7.2 can be recast in an alternative form by substituting the following, which recognizes the fact that $\Delta G^\circ_c = 0$ at T_m:

$${}^{0}T_m = \frac{{}^{0}\Delta H^\circ_c}{{}^{0}\Delta S^\circ_c} \quad (7.3)$$

$${}^{1}T_m = \frac{{}^{0}\Delta H^\circ_c + \Delta H^\circ_l}{{}^{0}\Delta S^\circ_c + \Delta S^\circ_l} \quad (7.4)$$

where ${}^{0}T_m$ and ${}^{1}T_m$ are the midpoints of the A ↔ B and AX ↔ BX transitions, respectively.

(2) An estimate of ${}^{A}\Delta C^\circ_{pb}$ was derived from empirical formulas which relate ΔC°_{pb} to the amounts of polar and nonpolar solvent-accessible surface areas (ASA) buried upon binding as evaluated from structural data. Such formulas have proven to give reasonable estimates of $\Delta C_p{}^\circ$ for binding in general (*33*) and for SH2−phosphopeptide interactions in particular (*31*, *40*). The structures used for ASA calculations were that of the Syk-tSH2−CD3-ϵ complex determined recently (*24*). Using the relationship reported by Spolar and co-workers (*41*), the calculated value for ${}^{A}\Delta C^\circ_{pb}$ by the ASA method is −209 cal mol^{-1} K^{-1}. Alternative values of ${}^{A}\Delta C^\circ_{pb}$ between −150 and −350 cal mol^{-1} K^{-1} (the asymptotic value of ΔC°_{pobs} in the low-temperature range of Figure 4) did not fundamentally alter the results of the fit. Thus, any inaccuracy in the ${}^{A}\Delta C^\circ_{pb}$ calculation is unlikely to significantly effect our parameter estimates.

Hence, as a result of the two approximations listed above, the parameters remaining to be determined are ${}^{A}T_{hb}$ and ${}^{A}T_{sb}$ which define ${}^{A}K_b(T)$, ΔH°_l and ${}^{1}T_m$ which define $K_l(T)$, and ${}^{0}\Delta H^\circ_c$ and ${}^{0}T_m$ which define ${}^{0}K_c(T)$. The former two sets of parameters are peptide-specific, and the latter set applies to the conformational change of the unligated protein.

RESULTS

Determination of Binding Constants. Binding constants for a dually phosphorylated ITAM peptide derived from the ITAM of the CD3-ϵ chain of the T cell receptor were determined by fluorescence titration by exploiting the change in intrinsic tryptophan fluorescence of the Syk tandem-SH2 domain upon ligation. Upon saturation with the CD3-ϵ ligand at 20 °C, a blue shift of approximately 10 nm in the fluorescence emission maximum was observed which was accompanied by ∼25% quenching at 340 nm. Representative titrations are shown in Figure 2. Binding association constants were determined from 4.5 to 30 °C and ranged from 1.24×10^7 M^{-1} (K_d = 80.9 nM) at the highest temperature to 5.54×10^7 M^{-1} (K_d = 18.0 nM) at the lowest temperature. Complete results with uncertainty estimates are depicted in Figure 3 and Table 1. As shown in Figure 3, K_{obs} exhibits only a modest temperature dependence.

Determination of Enthalpies of Binding and the Temperature Dependence of Thermodynamic Parameters. Results of calorimetric measurements of the enthalpies of binding of CD3-ϵ ITAM to Syk-tSH2 as a function of temperature are shown in Figure 4. ΔH°_{obs} is negative over the entire range of temperatures that was examined. Surprisingly, ΔH°_{obs} exhibits a nonlinear dependence on temperature, although the plot approaches linearity at the low-temperature limit. Thus, ΔC°_{pobs}, the first derivative of ΔH°_{obs} with respect to temperature, is temperature-dependent. Typically, $\Delta C_p{}^\circ$ is constant for protein folding and protein−ligand interactions over experimental temperature ranges (*42*, *43*). Exceptions

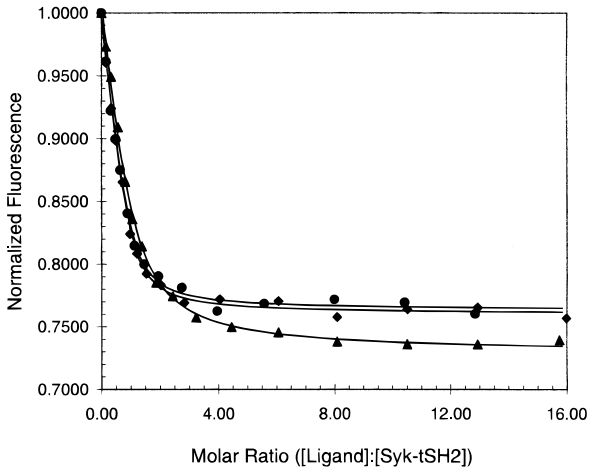

FIGURE 2: Representative fluorescence titrations. The fluorescence signal normalized for both protein concentration and initial fluorescence is shown as a function of the molar ratio of ligand (the CD3-ϵ peptide) to protein. For clarity, only three typical titrations at 15 (●), 20 (◆), and 30 °C (▲) are shown. Solid lines represent fits for the titrations; the resulting K_{obs} values are plotted in Figure 3.

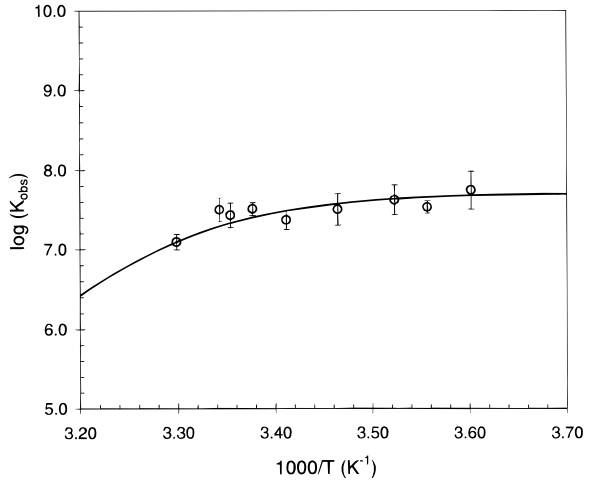

FIGURE 3: Temperature dependence of the binding constants for the CD3-ϵ peptide plotted as a van't Hoff plot. Error bars represent 95% confidence intervals as described in Materials and Methods. The solid line through the data is calculated from the results of the global analysis (see the Discussion) and describes the temperature dependence of K_{obs} according to eq 1.

have been noted for several processes, including calmodulin binding to peptide (*44*), IMP binding to IMP dehydrogenase (*34*), and other dehydrogenase−ligand interactions (reviewed in ref *35*). In each of these cases, the temperature-dependent ΔC_p° is attributed to the pre-existence of a temperature-dependent conformational equilibrium in one of the binding partners that is coupled to the binding process. This important observation leads us to propose that two conformers of unligated Syk-tSH2 exist in a binding-linked equilibrium, with one conformer predominating at the lowest temperatures studied and the other populated at higher temperatures (see the Discussion).

To assess the degree to which coupled temperature-dependent protonation equilibria could account for the curvature in the ΔH_{obs} data, a series of similar experiments were conducted in a buffer similar to the standard experimental buffer but where Pipes was substituted for Hepes. Pipes and Hepes have different ionization enthalpies (ΔH°_{ion} of Hepes is equal to 5.0 kcal/mol compared with a value of 2.6 kcal/mol for Pipes), and therefore, a coupled protonation event could be easily revealed from any difference observed between the experiments conducted in Hepes and those conducted in Pipes. The "Pipes" series of measurements were conducted at 10, 15, 20, and 25 °C. As shown in Figure 4, the observed binding enthalpies at all temperatures that were studied do not differ significantly from those measured in Hepes buffer, indicating that no protons are exchanged upon binding of the CD3-ϵ peptide to Syk-tSH2 under the solution conditions that were examined.

Given that ΔH°_{obs} is strongly dependent on temperature and that ΔG°_{obs} exhibits almost no temperature dependence, ΔS°_{obs} must also depend strongly on temperature in a manner that compensates for the temperature dependence of ΔH°_{obs}. This can be seen in the values of ΔS°_{obs} listed in Table 1. ΔS°_{obs} makes a strong favorable contribution to the observed binding free energy at the lowest temperatures (5−10 °C) while making a strong, unfavorable contribution at the highest temperatures (25−30 °C). Thus, the thermodynamics of binding at low temperatures resemble those of a rigid-body process, whereas at higher temperatures, they are more characteristic of an induced-fit process (*34*).

Determination of the On-Rate of Binding. To further examine the hypothesis, suggested by the unusual temperature dependence of ΔC°_{pobs}, that Syk-tSH2 exists as a mixture of two equilibrium conformers whose populations are affected by temperature, stopped-flow fluorescence was used to examine the binding kinetics for the CD3-ϵ peptide. In preliminary experiments conducted under pseudo-first-order conditions at 25 °C, a single exponential could be resolved for the first 5 s with a relaxation time constant that was proportional to the Syk-tSH2 and CD3-ϵ concentrations at all the concentrations that were investigated, with the fastest relaxation time being 7.2 ms (data not shown). The apparent second-order rate constant, k_{obs}, was determined to be 2.1×10^7 M^{-1} s^{-1} at 25 °C. A slower phase ($\tau \approx 60-120$ s) with a small amplitude was also present but could not be accurately resolved from photobleaching artifacts.

To determine whether the observed single exponential represents a combination of microscopic processes, i.e., two conformers binding in parallel with unresolvable rate constants, k_{obs} was measured as a function of temperature between 7.5 and 30.7 °C under conditions of excess ligand. The results are shown as an Arrhenius plot in Figure 5. According to the Arrhenius equation ($k = Ae^{-E_a/RT}$), a plot of log(k_{obs}) versus inverse temperature should be linear if k_{obs} represents a rate constant for a single microscopic process. The plot shown in Figure 5 is clearly not linear, although the low-temperature limit seems to approach linearity. As discussed below, this behavior can be explained by the same hypothesis suggested by the binding enthalpy data, i.e., that a single conformer of Syk-tSH2 is populated at low temperatures and one or more additional conformers become significantly populated as the temperature is raised (see the Discussion).

Temperature Dependence of the Fluorescence of Syk-tSH2 and the CD3-ϵ ITAM Complex. As a direct probe of the putative temperature-dependent conformational equilibrium, we examined the temperature dependence of the intrinsic fluorescence signal of Syk-tSH2 and its CD3-ϵ complex. Fluorescence intensity does not vary linearly with temper-

Table 1: Thermodynamic Parameters for CD3-ϵ Ligand Binding to Syk-tSH2 at Various Temperatures in Hepes at pH 7.5

T (°C)	n^a	log(K_{obs}) ($\times 10^8$ M^{-1})	$K_{d,obs}{}^b$ (nM)	ΔG°_{obs} (kcal/mol)	$\Delta H^\circ_{obs}{}^c$ (kcal/mol)	$T\Delta S^\circ_{obs}{}^d$ (kcal/mol)
4.5	1	7.74 ± 0.24	18.0 (8.1−28.0)	−9.83 ± 0.30	−1.69 (±0.76)^e	8.14 ± 0.82
7.5	2	7.53 ± 0.19	29.4 (16.7−42.0)	−9.70 ± 0.24	−2.56	7.14 ± 0.80
10	1	7.62 ± 0.20	23.8 (12.9−34.8)	−9.90 ± 0.26	−3.69	6.21 ± 0.80
15	3	7.50 ± 0.12	31.5 (22.6−40.4)	−9.90 ± 0.16	−5.90	4.00 ± 0.78
20	4	7.37 ± 0.08	42.9 (34.8−51.0)	−9.89 ± 0.11	−9.79	0.10 ± 0.77
23	2	7.51 ± 0.16	31.1 (24.4−49.8)	−10.18 ± 0.21	−13.3	−3.12 ± 0.79
25	1	7.43 ± 0.15	37.1 (24.4−49.8)	−10.15 ± 0.20	−15.8	−5.65 ± 0.79
26	1	7.50 ± 0.10	31.8 (24.6−38.9)	−10.27 ± 0.13	−17.5	−7.23 ± 0.77
30	3	7.10 ± 0.08	80.9 (66.2−95.7)	−9.84 ± 0.11	−23.8	−13.96 ± 0.77

[a] Number of titrations fit to the single K_{obs}. [b] Equal to $1/K_{obs}$. Numbers in parentheses are 95% confidence limits. The asymmetry results from fitting for log(K_{obs}) which has symmetric confidence limits. [c] ΔH°_{obs} values are interpolated from Figure 4 to temperatures at which K_{obs} values were determined. [d] Calculated from $T\Delta S^\circ_{obs} = \Delta H^\circ_{obs} - \Delta G^\circ_{obs}$. Uncertainty estimates propogated from values listed for ΔG°_{obs} and ΔH°_{obs}. [e] Error estimates are based on replicate measurements at representative temperatures; see Materials and Methods for details.

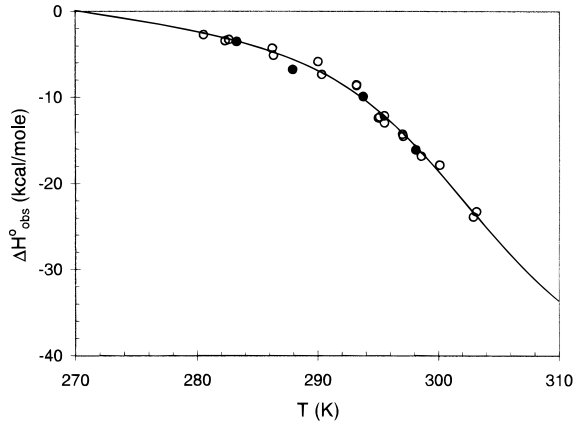

FIGURE 4: Calorimetric enthalpies of binding as a function of temperature. Estimated 95% confidence intervals for each point are ±0.76 kcal/mol and were determined as described in Materials and Methods. The solid line through the data represents the predicted curve from the global analysis and describes ΔH°_{obs} as a function of temperature according to eq 3. Data denoted with white symbols were obtained in Hepes buffer at pH 7.5, while data denoted with black symbols were obtained in Pipes buffer at pH 7.5.

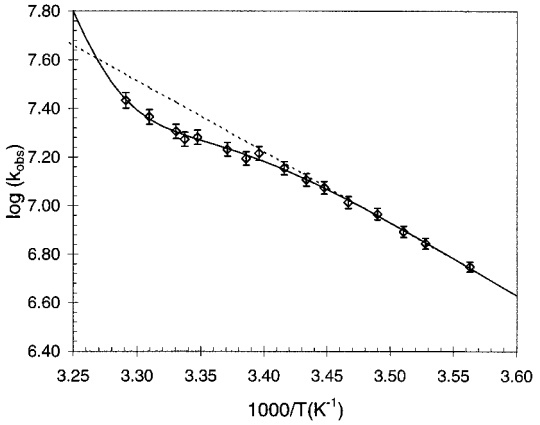

FIGURE 5: Apparent on-rates for binding of the CD3-ϵ ligand to Syk-tSH2 plotted as an Arrhenius plot (log k_{obs} vs inverse temperature). Error bars are 95% confidence limits derived from exponential fitting of the raw kinetic data. The dashed line represents a linear regression extrapolated from the four lowest-temperature data points and illustrates the failure of the simple Arrhenius equation to describe the data. The solid line represents a fit to eq 5 with the constraints and assumptions discussed in the text and is meant only to illustrate the adequacy of eq 5 in describing the data.

ature; however, we established that a van't Hoff-like plot of log(F_{obs}) versus $1/T$ for *N*-acetyltryptophanamide in the experimental buffer was linear between 4 and 50 °C (Figure 6). This is not surprising because static fluorescence is essentially an equilibrium process with the fluorescence intensity being proportional to the effective equilibrium constant governing the emission and competing relaxation processes. Therefore, we expected that a plot of log(F_{obs}) versus inverse temperature for a single conformer would be linear. Logarithmic plots for the unligated Syk-tSH2 and the CD3-ϵ complex were generated. The plot for unligated Syk-tSH2 exhibits a distinct curvature in the temperature range that was examined (5−33 °C), which was interpreted to indicate the presence of two or more conformers whose populations are affected by temperature. The log(F_{obs}) versus $1/T$ plot for the CD3-ϵ complex showed no deviation from linearity between 3.7 and 36 °C, which may indicate that the population of the CD3-ϵ-bound state of the protein is dominated by one conformer (see the Discussion).

Temperature Dependence of the Circular Dichroism Spectrum of Syk-tSH2. To further characterize the conformational transition between the low- and high-temperature conformers of Syk-tSH2, near-UV circular dichroism (CD) was used as a probe of tertiary structure. Spectra were taken from 305 to 270 nm at temperatures ranging from 10 to 30 °C; results are shown in Figure 7. These spectra are very similar; apparently, the conformational transition does not induce a major change in the near-UV CD spectrum. However, these results indicate that tertiary structure is maintained as the temperature is increased. Thus, the conformational change implicated by the evidence presented above is not due to a partial unfolding event, and the high-temperature conformer appears to be a native form of Syk-tSH2 as opposed to an intermediate or unfolded form.

DISCUSSION

Recognition of dually phosphorylated ITAM sequences by the tandem-SH2 domains of Syk family kinases is crucial to signaling in immune cells. In an effort to characterize these interactions, we first determined the structure of a complex of the tandem-SH2 domain of Syk bound to a dually phosphorylated ITAM derived from the ϵ chain of the T cell receptor (*24*). It was found that in the bound state, considerable flexibility in the relative orientation of the two SH2 domains is permitted. However, the significance of this conformational flexibility in solution remained undocu-

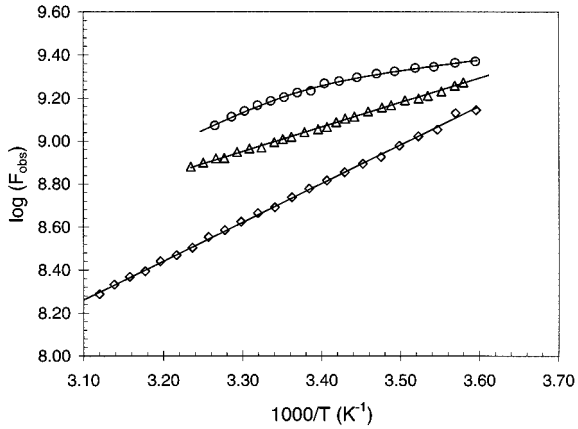

FIGURE 6: Fluorescence of Syk-tSH2 and its CD3-ϵ complex. The fluorescence signals of unligated Syk-tSH2 (○), the CD3-ϵ complex (△), and an *N*-acetyltryptophan control sample (◇) at varying temperature are plotted as log(F_{obs}) vs inverse temperature. Uncertainties associated with fluorescence readings based on multiple measurements were <0.8% of the raw fluorescence value, and error bars would be smaller than the plotted symbols. The solid line through the Syk-tSH2 (○) data represents a fit derived from the global analysis as described in the Discussion; the fluorescence as a function of temperature is described by eq 4. Solid lines through the Syk-tSH2−CD3-ϵ complex (△) and *N*-Ac-Trp data (◇) represent simple linear regression fits to the data, indicating that the fluorescence of a single population is adequately described by a straight line when plotted in this manner.

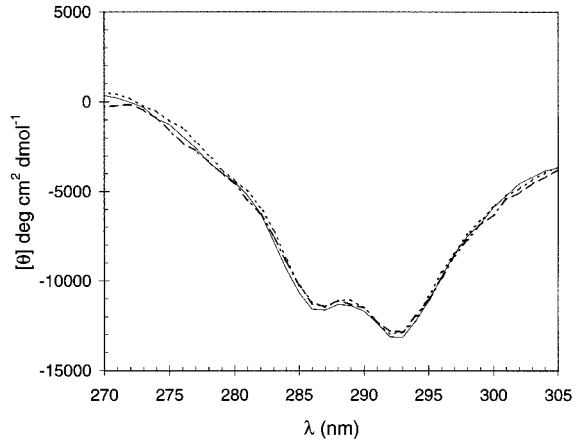

FIGURE 7: Near-UV circular dichroism spectra of Syk-tSH2 at 10 (- - -), 20 (—), and 30 °C (— - —).

mented. Moreover, it was unclear whether the observed structural flexibility was relevant to the free state of the protein. To answer some of these questions, the thermodynamics of binding of Syk-tSH2 to the peptide used in the crystallographic studies were investigated and found to be complicated by a linked process which could be attributed to a temperature-dependent conformational equilibrium such as the one presented in Scheme 1.

Evidence Supporting the Model of Scheme 1. The most compelling evidence for the two-conformer model of Scheme 1 is provided by the temperature dependence of the binding enthalpy (Figure 4) which shows an unusual curvature, indicating a temperature-dependent $\Delta C_{p\mathrm{obs}}^{\circ}$. At low temperatures, the variation of $\Delta H_{\mathrm{obs}}^{\circ}$ with temperature is nearly linear, and $\Delta C_{p\mathrm{obs}}^{\circ}$ is not large; the lower limit of $\Delta C_{p\mathrm{obs}}^{\circ}$ based on the three lowest temperature points is −349 cal mol^{-1} K^{-1}. At higher temperatures, the magnitudes of $\Delta C_{p\mathrm{obs}}^{\circ}$ increase dramatically, −1400 cal mol^{-1} K^{-1} at the highest temperatures that were studied. This behavior can be understood by examination of eq 3 and Scheme 1. Temperature induces a conformational change in one of the binding partners from A, which predominates at low temperatures, to B, which becomes populated at higher temperatures. When binding occurs at higher temperatures, the observed enthalpy is a composite of at least two exothermic components: one from the intrinsic binding enthalpy, the first term of eq 3, and one from the enthalpy of the coupled B → A transition multiplied by the fractional population of the B form, the second term of eq 3. The magnitude of the latter contribution to $\Delta H_{\mathrm{obs}}^{\circ}$ increases with temperature in a sigmoidal fashion. The coupled B → A transition may not be complete; that is, BX may be significantly populated at equilibrium, in which case the third term of eq 3 becomes significant. The degree to which the transition is complete may depend on the identity of the ligand as well as on temperature.

The assignment of the conformational change to the protein results from the temperature dependence of the fluorescence of unligated Syk-tSH2. As discussed in the Results, a plot of log(F_{obs}) versus 1/T was expected to be linear for a single conformer. The plot in Figure 6 for the unligated Syk-tSH2 approaches linearity between 5 and 12 °C (3.5−3.6 on the 1000/T axis), but exhibits a distinct curvature at higher temperatures. This is consistent with the predominance of the A form of Syk-tSH2 at low temperatures and an equilibrium between the A and B conformers at higher temperatures. The log(F_{obs}) versus 1/T plot for the CD3-ϵ complex (Figure 6) is linear over the entire temperature range that was examined as indicated by the solid linear regression fit. The good agreement of this linear fit to the data is consistent with the hypothesis that ligand binding stabilizes the AX form; the absence of curvature may indicate that BX is only weakly populated and that the linkage constant, K_{l}, for the CD3-ϵ peptide ($K_{\mathrm{l}\epsilon}$) is close to zero (see Scheme 1) over the investigated temperature range.

The nonlinear Arrhenius plot for the kinetics of binding of the CD3-ϵ peptide to Syk-tSH2 shown in Figure 5 is further support for the model presented in Scheme 1. Examination of eq 5 shows that the Arrhenius plot for the two-conformer model would approach linearity toward the low-temperature limit where binding to the A form predominates and the high-temperature limit where binding to the B form predominates; the middle region would exhibit a curvature representing a mixing of the A + x → AX and B + x → BX reactions as a result of the A ↔ B conformational equilibrium. This is precisely what was observed for the binding of CD3-ϵ to Syk-tSH2. Previous examples of this type of kinetic behavior have been reported and interpreted as evidence of temperature-dependent conformational changes (*45*−*47*).

Thermodynamic and Kinetic Parameters for CD3-ϵ ITAM Binding. Global nonlinear least-squares fitting was used to obtain quantitative estimates of the parameters defining the equilibrium constants of Scheme 1 as functions of temperature. The two approximations listed in Theory helped reduce the number of parameters that needed to be determined. Moreover, since the BX form is apparently either unpopulated or weakly populated, $K_{\mathrm{l}\epsilon}$ was set to zero. We should note that setting $K_{\mathrm{l}\epsilon}$ to a temperature-independent value of 0.05 (the upper limit value for $K_{\mathrm{l}\epsilon}$ consistent with the uncertainties in the fluorescence data), corresponding to an

Table 2: Results of Simultaneous Nonlinear Least-Squares Fitting of Data for Binding of the CD3-ϵ Peptide to Syk-tSH2

data included in fit	ΔH°_{obs}, K_{obs}, F_{obs}
standard deviation of fit	0.667
parameters fitted directly	
ΔC_{pb}° (cal mol^{-1} K^{-1})[a]	−209
$^{A}T_{hb}$ (K)	270.9 ± 4.7
$^{A}T_{sb}$ (K)	320.4 ± 5.9
$^{0}\Delta H_{c}^{\circ}$ (kcal/mol)	32.3 ± 3.1
$^{0}T_{m}$ (K)	302.6 ± 1.4
parameters calculated from fit	
$^{A}K_{d}$ (nM)[b-d]	32.1 (19.8−52.1)
$^{A}\Delta H_{b}^{\circ}$ (kcal/mol)	−5.68 ± 1.19
$^{A}\Delta S_{b}^{\circ}$ (cal mol^{-1} K^{-1})	15.0 ± 4.3
$^{0}K_{c}$[b,d]	0.50 (0.37−0.69)
$^{0}\Delta S_{c}^{\circ}$	107.2 ± 51

[a] Parameter was fixed to a calculated value as described in the Discussion. [b] Numbers in parentheses are 95% confidence limits; asymmetry is a result of fitting for the logarithm of the indicated value, which has symmetric confidence limits. [c] Dissociation constant of the A form of the complex. [d] Calculated at 25 °C.

~5% population of the BX state, did not significantly affect the fit to the data. The results of the fit are shown in Table 2; fitted curves for each set of data are shown in Figures 3, 4, and 6. The agreement of the fitted curves to the data is convincing, demonstrating that Scheme 1 is sufficient to describe the linked binding and conformational processes.

Values for K_d and other variables calculated from the intrinsic thermodynamic parameters interpolated to 25 °C are shown in Table 2. The intrinsic T_h for binding to the A form is <0 °C, indicating that binding is exothermic at all experimentally accessible temperatures. $^{A}T_{sb}$ is greater than the experimental temperature window, indicating that the entropy of binding to the A form is also favorable at all the temperatures that were studied. It is estimated that the A ↔ B isomerization takes place with an enthalpy (ΔH_c°) of 32.3 ± 3.1 kcal/mol and a transition centered at a T_m of 302.6 ± 1.4 K, indicating that the conformational change takes place over a broad temperature range. At 15 °C, the B form is 5% populated; at 48 °C, well above the temperatures we were able to access experimentally, the transition is only 95% complete. In fact, the breadth of the A ↔ B transition precluded direct measurement of the transition by differential scanning calorimetry (results not shown). The positive enthalpy could indicate that the transition from A to B resembles an unfolding event; however, this is not the case. The CD data presented in Figure 7 indicate that the high-temperature conformer of Syk-tSH2 is a native form of the protein.

The kinetic data (Figure 5) were not incorporated into the global analysis because determination of the spectroscopic weighting factors in eq 5 would be difficult. However, to show that the nonlinear behavior observed in the Arrhenius analysis is qualitatively consistent with the proposed model, the data of Figure 5 were fit to eq 5 with the assumption that the fluorescence values of the two conformers are similar with respect to absolute magnitude, i.e., that $W_A = W_B$. The solid line of Figure 5 represents the fit as described. It is clear from the quality of the fit that the variation of k_{obs} with temperature supports the model presented in Scheme 1. The value for observed second-order rate constant, k_{obs}, for binding of the CD3-ϵ ligand to Syk-tSH2 at 25 °C is 2.1 × 10^7 M^{-1} s^{-1}, a typical rate constant for protein−protein associations (*48*). As discussed, this represents an average of two intrinsic rate constants that are apparently similar in magnitude. The kinetics suggest that the two forms of Syk-tSH2 bind to the CD3-ϵ ligand and that the off-rate for CD3-ϵ peptide binding to the B form is faster than that for binding to the A form. As a result, a shift in the conformational distribution occurs after the kinetic binding step. Thus, although BX may bind transiently, it is apparently not populated at equilibrium. This shift in the conformational distribution is likely to be responsible for the low-amplitude slow phase described in the Results.

Conclusion. Does the conformational change described here have implications for the role of Syk in vivo? It is possible that a ligand-linked conformational change could regulate the enzymatic activity of the kinase domain. This would be consistent with reports that suggest that ligation is linked to conformation and activity in the full-length Syk enzyme (*49*, *50*). However, a second possible role for the conformational transition may be that it imparts an inherent flexibility to Syk-tSH2 so that it can accommodate a variety of binding partners.

The recent report of the X-ray crystal structure of the Syk-tSH2−CD3-ϵ complex suggested that conformational flexibility may be a salient feature of Syk-tSH2 binding to ITAMs (*24*). This structure contains six Syk-tSH2 molecules per asymmetric unit, providing six "snapshots" of the complex. Among these six molecules, significant variation in the relative orientation of the two SH2 domains was observed such that the two extreme structures differ by an 18° rotation of the C-terminal SH2 domain about its αB helix axis relative to the N-terminal SH2, with concomitant changes in the ligand and inter-SH2 regions (see Figure 1B). The SH2 domains themselves move as rigid bodies that deviate little from the canonical SH2 domain structure (*51*). Removal of the structural constraints imposed by the ligand may allow even larger variation in the relative orientation of the two SH2 domains. Thus, we interpret the structural data to indicate that motions of the sort observed in the crystal structure can take place in the unbound state without prohibitive changes in energy. The energy levels of regions of conformational space that are sampled by such motions could be altered by the temperature, the ligation state, and the identity of the ligand, consistent with the model we present here.

Conformational flexibility in Syk-tSH2 may be necessary for it to fulfill its role as a player in signal transduction pathways initiated by a variety of receptors, including B and T cell antigen receptors (*1*, *3*), Fc class I and III receptors (*2*), FcγRIIA receptor (*21*, *52*), and colony-stimulating factor receptor (*17*), as well as pathways mediated by integrins (*20*) and G protein-coupled receptors (*22*). In some of these pathways, ITAMs, if required, have yet to be identified, but in at least two cases, those for colony-stimulating factor receptor and FcγRIIA, the putative ITAMs possess primary structures that deviate considerably from canonical [Yxx(L/I)-$x_{7/8}$-Yxx(L/I)] ITAMs in that they contain four and five additional residues, respectively, between phosphotyrosines (*17*, *23*). Therefore, it seems plausible that the SH2 domains of Syk adopt a variety of relative orientations to accommodate diverse ligands. We believe that such adaptability results in the complex thermodynamics we report here and the structural flexibility reported previously (*24*). Certainly,

this flexibility ought to be considered in the design of signaling inhibitors that act via the tandem-SH2 domain of Syk. A rigid inhibitor may act against only a subset of the conformations that are available to the tandem-SH2 domain.

It is not known how the presence of the linker region between the tandem-SH2 domain and the kinase domain, or of the kinase domain itself, might affect the conformational change demonstrated in this report. However, the conformational transition that we describe is indicative of at least two energy minima corresponding to functional structures. While other parts of the protein or other factors in vivo may influence the level of these energy minima, it seems unlikely that they would be eliminated altogether. Furthermore, the concordance of the results of this study and those of the X-ray crystal structure with the database of biological data suggesting functional ubiquity for Syk is a good indicator that flexibility in the tandem-SH2 domain has significant biological implications.

ACKNOWLEDGMENT

We thank Drs. T. M. Lohman and C. Frieden for the use of the fluorometers and stopped-flow apparatus, Dr. J. I. Gordon for the use of the Microcal calorimeter, and Drs. K. B. Hall, R. Bhatnagar, A. Vindigni, J. M. Bradshaw, A. Kozlov, and A. Herr for comments. We are particularly indebted to Dr. T. M. Lohman for valuable comments and insight.

REFERENCES

1. Chan, A. C., and Shaw, A. S. (1995) *Curr. Opin. Immunol. 8*, 394−401.
2. Daëron, M. (1997) *Annu. Rev. Immunol. 15*, 203−234.
3. Kurosaki, T. (1997) *Curr. Opin. Immunol. 9*, 309−318.
4. Reth, M., and Wienands, J. (1997) *Annu. Rev. Immunol. 15*, 453−479.
5. Costello, P. S., Turner, M., Walters, A. E., Cunningham, C. N., Bauer, P. H., Downward, J., and Tybulewicz, V. L. (1996) *Oncogene 13*, 2595−2605.
6. Crowley, M. T., Costello, P. S., Fitzer-Attas, C. J., Turner, M., Meng, F., Lowell, C., Tybulewicz, V. L., and DeFranco, A. L. (1997) *J. Exp. Med. 186*, 1027−1039.
7. Zhang, J., Berenstiein, E. H., Evans, R. L., and Siraganian, R. P. (1996) *J. Exp. Med. 184*, 71−80.
8. Cheng, A. M., and Chan, A. C. (1997) *Curr. Opin. Immunol. 9*, 528−533.
9. Cambier, J. C. (1995) *J. Immunol. 152*, 3281−3285.
10. Reth, M. (1989) *Nature 338*, 383−385.
11. Bu, J. Y., Shaw, A. S., and Chan, A. C. (1995) *Proc. Natl. Acad. Sci. U.S.A. 92*, 5106−5110.
12. Chen, T., Repetto, B., Chizzonite, R., Pullar, C., Burghardt, C., Dharm, E., Zhao, Z., Carroll, R., Nunes, P., Basu, M., Danho, W., Visnick, M., Kochan, J., Waugh, D., and Gilfillan, A. M. (1996) *J. Biol. Chem. 271*, 25308−25315.
13. Isakov, N., Wange, R. L., Burgess, W. H., Watts, J. D., Aebersold, R., and Samelson, L. E. (1995) *J. Exp. Med. 181*, 375−380.
14. Iwashima, M., Irving, B. A., van Oers, N. S., Chan, A. C., and Weiss, A. (1994) *Science 263*, 1136−1139.
15. Kurosaki, T., Johnson, S. A., Pao, L., Sada, K., Yamamura, H., and Cambier, J. C. (1995) *J. Exp. Med. 182*, 1815−1823.
16. Kong, G. H., Bu, J. Y., Kurosaki, T., Shaw, A. S., and Chan, A. C. (1995) *Immunity 2*, 485−492.
17. Corey, S. J., Burkhardt, A. L., Bolen, J. B., Geahlen, R. L., Tkatch, L. S., and Tweardy, D. J. (1994) *Proc. Natl. Acad. Sci. U.S.A. 91*, 4683−4687.
18. Higuchi, M., Asao, H., Tanaka, N., Oda, K., Takeshita, T., and Sugamura, K. (1997) *Leukemia 11*, 416−417.
19. Gao, J., Zoller, K. E., Ginsberg, M. H., Brugge, J. S., and Shattil, S. J. (1997) *EMBO J. 16*, 6414−6425.
20. Lin, T. H., Rosales, C., Mondal, K., Bolen, J. B., Haskill, S., and Juliano, R. L. (1995) *J. Biol. Chem. 270*, 16189−16197.
21. Yanaga, F., Poole, A., Asselin, J., Blake, R., Schieven, G. L., Clark, E. A., Law, C. L., and Watson, S. P. (1995) *Biochem. J. 311*, 471−478.
22. Wan, Y., Kurosaki, T., and Huang, X. Y. (1996) *Nature 380*, 541−544.
23. Chacko, G. W., Brandt, J. T., Coggeshall, K. M., and Anderson, C. L. (1996) *J. Biol. Chem. 271*, 10775−10781.
24. Fütterer, K., Wong, J., Grucza, R. A., Chan, A. C., and Waksman, G. (1998) *J. Mol. Biol. 281*, 523−533.
25. Lemmon, M. A., and Ladbury, J. E. (1994) *Biochemistry 33*, 5070−5076.
26. Ladbury, J. E., Lemmon, M. A., Zhou, M., Green, J., Botfield, J., and Schlessinger, J. (1995) *Proc. Natl. Acad. Sci. U.S.A. 92*, 3199−3203.
27. Ladbury, J. E., Hensmann, M., Panayotou, G., and Campbell, I. D. (1996) *Biochemistry 35*, 11062−11069.
28. Lemmon, M. A., Ladbury, J. E., Mandiyan, V., Zhou, M., and Schlessinger, J. (1994) *J. Biol. Chem. 269*, 31653−31658.
29. Charifson, P. S., Shewchuk, L. M., Rocque, W., Hummel, C. W., Jordan, S. R., Mohr, C., Pacofsky, G. J., Peel, M. R., Rodriguez, M., Sternbach, D. D., and Consler, T. G. (1997) *Biochemistry 36*, 6283−6293.
30. McNemar, C., Snow, M. E., Windsor, W. T., Prongay, A., Mui, P., Zhang, R., Durkin, J., Le, H. V., and Weber, P. C. (1997) *Biochemistry 36*, 10006−10014.
31. Bradshaw, J. M., Grucza, R. A., Ladbury, J. E., and Waksman, G. (1998) *Biochemistry 37*, 9083−9090.
32. Bradshaw, J. M., and Waksman, G. (1998) *Biochemistry 37*, 15400−15407.
33. Spolar, R. S., and Record, M. T., Jr. (1994) *Science 263*, 777−784.
34. Bruzzese, F. J., and Connelly, P. R. (1997) *Biochemistry 36*, 10428−10438.
35. Fisher, H. F. (1988) *Adv. Enzymol. 61*, 1−45.
36. Lawrence, D. S., and Niu, J. (1998) *Pharmacol. Ther. 77*, 81−114.
37. Moriya, K., Rivera, J., Odom, S., Sakuma, Y., Muramato, K., Yoshiuchi, T., Miyamoto, M., and Yamada, K. (1997) *Proc. Natl. Acad. Sci. U.S.A. 94*, 12539−12544.
38. Gill, S. C., and von Hippel, P. H. (1989) *Anal. Biochem. 182*, 319−326.
39. Cousins-Wasti, R. C., Ingraham, R. H., Morelock, M. M., and Grygon, C. A. (1996) *Biochemistry 35*, 16746−16752.
40. Waksman, G., Shoelson, S. E., Pant, N., Cowburn, D., and Kuriyan, J. (1993) *Cell 72*, 779−790.
41. Spolar, R. S., Livingstone, J. R., and Record, M. T., Jr. (1992) *Biochemistry 31*, 3947−3955.
42. Gomez, J., and Freire, E. (1995) *J. Mol. Biol. 252*, 337−350.
43. Gomez, J., Hilser, J. V., Xie, D., and Friere, E. (1995) *Proteins: Struct., Funct., Genet. 22*, 404−412.
44. Wintrode, P. L., and Privalov, P. L. (1997) *J. Mol. Biol. 256*, 1050−1062.
45. Allen, B., Blum, M., Cunningham, A., Tu, G. C., and Hofmann, T. (1990) *J. Biol. Chem. 265*, 5060−5065.
46. Biosca, J. A., Travers, F., Hillaire, D., and Barman, T. E. (1984) *Biochemistry 23*, 1947−1955.
47. Morpeth, F. F., and Massey, V. (1982) *Biochemistry 21*, 1307−1312.
48. Northrup, S. H., and Erickson, H. P. (1992) *Proc. Natl. Acad. Sci. U.S.A. 89*, 3338−3342.
49. Kimura, T., Sakamoto, H., Apella, E., and Siraganian, R. P. (1996) *Mol. Cell Biol. 16*, 1471−1478.
50. Shiue, L., Zoller, M. J., and Brugge, J. S. (1995) *J. Biol. Chem. 270*, 10498−10502.
51. Kuriyan, J., and Cowburn, D. (1997) *Annu. Rev. Biophys. Biomol. Struct. 26*, 259−288.
52. Matsuda, M., Park, J. G., Wang, D. C., Hunter, S., Chien, P., and Schreiber, A. D. (1996) *Mol. Biol. Cell. 7*, 1095−1106.

BI9829938